Available online at www.sciencedirect.com
SCIENCE DIRECT®
Journal of Computational Physics 198 (2004) 617–627
JOURNAL OF COMPUTATIONAL PHYSICS
www.elsevier.com/locate/jcp

Arbitrary-pressure chemical vapor deposition modeling using direct simulation Monte Carlo with nonlinear surface chemistry

Husain A. Al-Mohssen, Nicolas G. Hadjiconstantinou *

Mechanical Engineering Department, Massachusetts Institute of Technology, 77 Massachusetts Avenue, Cambridge, MA 02139, USA

Received 9 September 2003; received in revised form 19 January 2004; accepted 21 January 2004
Available online 6 March 2004

Abstract

We present a methodology for simulating chemical vapor deposition (CVD) which uses the direct simulation Monte Carlo (DSMC) method to capture gaseous phase transport in a wide Knudsen (Kn) range. This work bridges different CVD simulation methods developed for the Navier–Stokes ($Kn \to 0$) and ballistic ($Kn \to \infty$) regimes. Our methodology incorporates a nonlinear surface chemistry model as well as a level set based profile evolution formulation which accurately captures complex boundary evolution, and is capable of accurately predicting surface growth for arbitrary complex geometries and surface chemistry for a wide range of Knudsen numbers. The proposed approach is validated by comparing its predictions to existing numerical results in the ballistic ($Kn \to \infty$) and diffusive ($Kn \ll 1$) regimes.

1. Introduction

Chemical vapor deposition (CVD) is a process of considerable practical importance [11]. Reliable simulation techniques can reduce production costs and improve product quality by reducing the trial and error associated with process optimization while keeping the need for costly experimental facilities to a minimum. Although such simulation techniques exist for the limiting cases when the molecular mean free path is much smaller or larger than the characteristic feature scale, satisfactory solutions which include arbitrary surface chemistry and level set surface evolution models for the more general (and considerably more challenging) problem of arbitrary mean free path do not exist. This paper reports on the development of such a method.

Gaseous transport above the feature surface plays a key role in determining the shape and physical properties of the deposited layer. A key parameter in characterizing gaseous transport is the ratio of the

* Corresponding author.
E-mail address: ngh@mit.edu (N.G. Hadjiconstantinou).

0021-9991/$ - see front matter © 2004 Elsevier Inc. All rights reserved.
doi:10.1016/j.jcp.2004.01.018

mean free path of the gas molecules to a characteristic surface dimension known as the Knudsen number Kn [2] . In this work the Knudsen number was defined as $Kn = \lambda/L$, where L is the initial trench mouth width. At low values of the Knudsen number ($Kn \to 0$), linear gradient transport holds and the standard multi-species Navier–Stokes (NS) equations accurately predict the flow characteristics [6,7]. At the other extreme ($Kn \to \infty$), no gas–gas collisions take place and transport is ballistic [1,4,5]. In the regime $0.1 \lesssim Kn \lesssim 10$ (known as the transition regime), no simplifying assumptions can be made and only the full Boltzmann equation accurately describes the transport [2,3]. Our methodology uses the direct simulation Monte Carlo (DSMC), a molecular simulation method shown to provide accurate solutions of the Boltzmann equation [27], to provide accurate description of gaseous transport in all Knudsen regimes. However, it should be noted that in the $Kn \to 0$ limit solutions based on the Navier–Stokes description are more practical and significantly more efficient [2].

Previous attempts to model CVD using the DSMC method [9–12] suffer from one or more of deficiencies such as, crude surface evolution models, crude DSMC implementations, high statistical scatter and lack of verification. This last consideration is, in fact, very important since a number of simplifying assumptions is made when developing these simulation models and especially after considering the fact that previous approaches either predict trends that are inconsistent with solutions in the $Kn \to 0$ or $Kn \to \infty$ regimes, or make use of simplifications that are too crude. A simple Monte Carlo approach based on a random walk model has also been proposed [8]; although such a model may be sufficiently accurate for some purposes, the approximations involved make it unclear whether it can be reliably used throughout the entire Knudsen range.

In this paper we discuss our approach towards developing a reliable CVD model based on DSMC which incorporates for the first time both a nonlinear surface chemistry and a level set surface evolution model. The surface chemistry and level set approaches are briefly described in Section 2. Moreover, our methodology is extensively tested and is shown to capture the predictions of established solution methods in the $Kn \ll 1$ and $Kn \to \infty$ limits. In the absence of transition-regime experimental data suitable for validation purposes, the above tests form an alternative numerical validation procedure (recall that DSMC is known [2] to correctly capture transport in all Knudsen regimes).

Our work follows [1] in assuming that gas phase chemistry is negligible, although methods of incorporating homogeneous reactions in the DSMC transport model have been developed [2,24]. Surface chemistry is typically modeled through the use of a *sticking coefficient* (Sc), defined as the probability that a molecule colliding with the reactive surface is absorbed and reaction follows. Previous transition regime models have usually used a sticking coefficient that is constant in space (all points on the surface have the same Sc) and time, despite ample evidence to the contrary [13]. In our work we have developed and incorporated a variable sticking coefficient concept appropriate for DSMC.

Collisions between particles and the evolving growth surface are handled by an algorithm that decouples the interface discritization size from the DSMC timestep. The algorithm is described in Section 2.1.

Another key challenge in CVD modeling is finding methods to robustly and efficiently represent and model feature surfaces in both two and three dimensions. To date, transition regime CVD models have used fairly basic representations of the deposition film that are either unphysical or not easily extended to three dimensions. In this work we capture film growth through a level set approach that avoids many of the disadvantages of simpler approaches (for a discussion see [19]).

2. Outline of methodology

A key typical assumption in computational CVD studies is that the gas transport characteristic timescale is significantly shorter than the timescale associated with the deposition boundary movement. Consequently, the deposition process can be split into two distinct steps, namely the calculation of the deposition

rate caused by the gas transport and the evolution of the growth surface. The following sections outline the major components of these sub-models; further details (along with implementation details and a discussion of some of the caveats) can be found in [14].

2.1. DSMC gas transport and deposition model

DSMC was invented by Bird in the 1960s as a method of solving the Boltzmann equation for a wide variety of conditions [2] and was recently proven to provide accurate solutions of this equation in the limit of infinitesimal discretization. The DSMC method is fairly well documented (see, for example [2,15,16]); as a result, we will only discuss aspects of our implementation that are special or non-standard.

Fig. 1 shows a sketch of the domain, DSMC cell grid and domain boundaries. The collision cells are rectangular and of equal size, while the deposition surface is discretized into short straight segments of an arbitrary length and number. In the figure, the initial boundary is shown as well as a schematic of the evolving boundary after finite time. Our discretization approach was chosen because it affords great flexibility in developing an efficient method that can be applied to a wide range of Knudsen numbers. Because the cell linear size (Δx) and DSMC timestep (Δt) are not coupled to the growth surface representation, they can be chosen to achieve the best compromise between efficiency and accuracy ($\Delta x \simeq \lambda/3$ and $\Delta t \simeq \lambda/(3c_0)$) [28–30], while the growth surface discretization can be made as fine as desired. Here λ is the mean free path and c_0 is the most probable molecular speed.

Collisions between particles and the growth surface are treated on an segment-by-segment basis while the excluded volume of the DSMC cells covered by the growing surface is calculated by a Monte Carlo hit and miss integration (subrandom [31] or even trapezoidal integration routines can also be used). Avoiding the significant bookkeeping task of processing particle collisions with the growth surface using cells that are

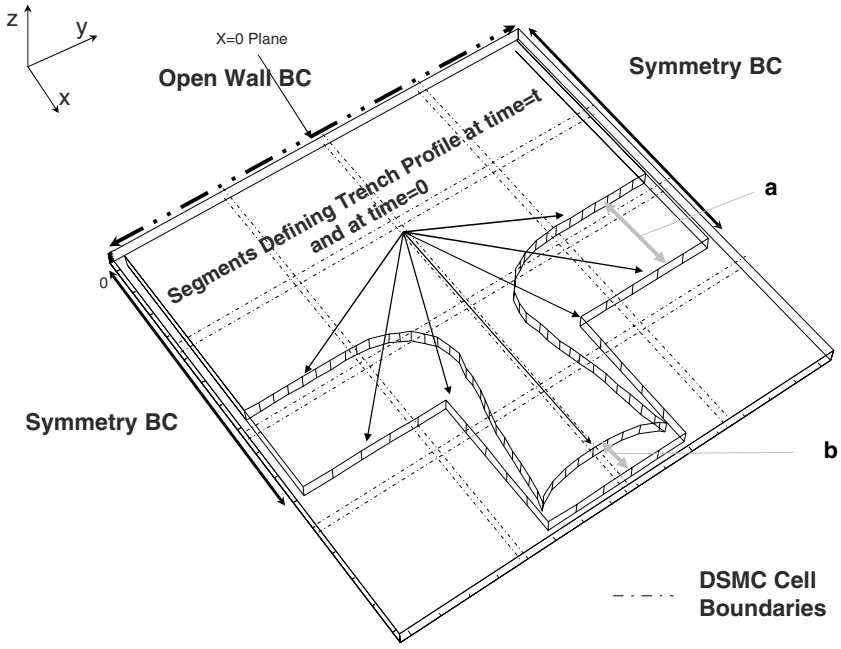

Fig. 1. Schematic of the simulation domain and boundary conditions. A cyclic (periodic) boundary condition is also applied in the z-direction to simulate the effect of an infinite trench.

conforming with the growth surface is achieved by assigning to each DSMC cell a number, $d_{\min}$, equal to the distance of the cell to the closest point on the deposition surface (corrected for the cell finite size). Particles are then only checked for collisions with the deposition surface if they travel a distance greater than $d_{\min}$ of the cell they originated from. An additional advantage of this approach is that it does not place a limit on the size of the DSMC timestep as in the case of schemes that check particles only within cells which are in contact with the surface.

The gas enters the simulation domain through an "open wall" boundary condition at the $x = 0$ plane. This boundary condition essentially matches the simulation to an infinite reservoir ($x < 0$) of a specified number density, composition, average velocity and temperature. Particles entering the domain are initialized using a Maxwell–Boltzmann distribution with zero mean velocity; a Chapman–Enskog distribution can also be used if exact coupling to an external field is required [26].

A periodic boundary condition is applied in the z-direction to simulate an infinitely long trench. The other domain boundaries are defined by the trench and symmetry boundary conditions at the ends of the domain. The symmetry boundary condition is applied by specularly reflecting gas particles that collide with the symmetry boundaries. Finally, our implementation allows for an arbitrary number of gaseous species.

Gas particles in the domain are moved using the standard DSMC advection schemes. The treatment of particles colliding with the deposition surface involves the absorption with the sticking coefficient probability Sc; the value of Sc is determined by the chemistry model as explained in Section 2.2.

In addition to the standard statistics collected in DSMC for the measurement of the usual physical variables of interest (flow, speed, concentration, temperature, etc.), statistics are collected for the number of particles that collide with the growth surface and the number of particles that stick to the surface. These are later used to infer the partial pressure of each species as well as the deposition rate as a function of location along the growth surface.

2.2. Chemistry model

Our nonlinear chemistry model follows the typical approach of controlling the reaction rate at the surface through a sticking coefficient. In our implementation the sticking coefficient varies as a function of space and time such that the local reaction rate is determined by the local conditions and their effect on the chemistry model. Although similar approaches have been used in diffusive [6,7] or ballistic studies [1,4], DSMC studies have typically been limited to a globally constant sticking coefficient.

To illustrate our implementation, let us assume that gases A and B react with a reaction rate $\mathscr{R}_A$ given by

$$\mathscr{R}_A = f[T, pp_A, pp_B, pp_D, \ldots] \tag{1}$$

in a reaction of the form

$$A + \beta B \rightarrow C(s) + \delta D, \tag{2}$$

where C is the deposited solid and D is a gaseous byproduct. Here pp_j is the partial pressure of species j, and $\mathscr{R}_B = \beta \mathscr{R}_A$. To implement this form of reaction in our "discrete" simulation we proceed by "splitting" the reaction equation (2) into two equations that involve only one of the reactants, that is,

$$A \rightarrow \frac{\gamma}{2} C(s) + \frac{\delta}{2} D \tag{3}$$

and

$$B \rightarrow \frac{\gamma}{2\beta} C(s) + \frac{\delta}{2\beta} D. \tag{4}$$

The partial pressures used in (1) are typically [1,17] inferred from the average number of particles that intersect each wall segment. Referring to one molecular species, the local number density can be approximated by

$$n = \frac{4g}{\bar{c}}, \tag{5}$$

where g is the flux of particles at the segment of interest, $\bar{c} = \sqrt{8kT/\pi m}$ is the mean molecular speed, k is Boltzmann's constant, T is the temperature and m is the molecular mass. Using the ideal gas law we can thus relate the partial pressures to the particle flux by

$$pp = \frac{4gRT}{\bar{c}}, \tag{6}$$

where $R = k/m$ is the gas constant for the particular species of interest. This equation along with (1) allows us to find the local reaction rate at each segment which in turn allows us to calculate the sticking coefficient from

$$Sc[\text{segment}(j), \text{species}(i)] = \frac{\mathscr{R}[j,i]}{g[j,i]}. \tag{7}$$

Byproduct transport is accounted for by creating byproduct particles in a ratio consistent with the splitting of (2). For example, in Reaction (3), $\delta/2$ particles of species D are created every time a particle of species A is adsorbed and likewise $\delta/2\beta$ particles of D are created each time species B is consumed. The new species are introduced in the domain at the point that the reacting particle hits the surface and they are moved for the balance of the timestep duration after the original particle reached the segment. When the number of byproduct species is not an integer, a byproduct particle is created with a probability equal to the fractional part of the number of particles created.

The deposition rate is calculated by either tracking the number of particles of each species that is absorbed into the deposition surface, or from Eq. (1) via the partial pressures generated from the number of particle collisions at each segment. The latter method gives much less noisy results particularly when the sticking coefficient is low.

A number of assumptions have been made in calculating the sticking coefficients that may not always hold. Most notable is the assumption of an equilibrium gas distribution that results in Eqs. (5) and (6) that we use above. In spite of this, the method is able to give correct results in many different cases and in particular it has been verified at high Knudsen numbers [1,17] where gas particle velocity distributions may deviate significantly from the equilibrium distribution. This is probably because the reaction rate (1) is really a function of the number of molecules that arrive at the surface which is subsequently converted to partial pressure using Eq. (6). We also find that our method is insensitive to the way Eq. (2) is split as long as the species balance is obeyed in an average sense.

2.3. Level set implementation

The basic idea behind the level set method is to regard the moving boundary as a constant-value (zero) contour of the function $\phi[t,x,y]$ which is defined on all points of the computational domain, that is at every point our evolving curve can go. A time-dependent partial differential equation governs ϕ and this determines the movement of the contour boundary. This method was pioneered by Osher and Sethian [18] and has been successfully used in modeling boundaries in a variety of different fields including deposition, image processing, combustion and many others [19]. There are a number of advantages in using LS to represent boundaries in CVD modeling, including the ability to deal with arbitrary topologies and their considerably less challenging extension to three dimensions [19].

In two dimensions, the equation governing the evolution of ϕ is

$$\frac{\partial\phi[t,x,y]}{\partial t} + F[x,y]|\nabla\phi[t,x,y]| = 0, \tag{8}$$

where $F[x,y]$ is a function that determines the velocity at which the boundary moves normal to itself. In the solution, ϕ is initialized as the distance to the closest point on the curve with a positive or negative sign depending on whether the point is inside or outside the curve, respectively.

The level set profile simulator is linked to our DSMC code through the following steps:

1. Initialize $\phi[t,x,y]$ as the signed distance function from the initial boundary curve γ^t and set $t=0$.
2. Run DSMC using γ^t and record the flux rate at each segment.
3. Use the flux rate data to build $F[x,y]$. This is called the extension problem and is explained in detail in [14,19,20].
4. Solve for $\phi[t+\Delta t_{\text{step}},x,y]$ (Δt_{step} is time between calls to DSMC) using the numerical scheme outlined in [19,21].
5. Use a contour extracting program to get γ^t from $\phi[t+\Delta t_{\text{step}},x,y]$.
6. Increment t by Δt_{step}, and repeat steps 2–6 until $t=t_{\text{final}}$.

3. Results

In this section we present and discuss some of our results. Our objective is to compare our method predictions with benchmark published results but also to investigate CVD in the transition regime for which few results exist. A considerable amount of *reliable* results involving non-trivial surface chemistry exists in the $Kn\to\infty$ limit. We use a variety of these results to validate our work. We additionally obtain results for low Knudsen numbers ($Kn=0.03$) based on the diffusion equation. This provides another independent validation for our method. Since DSMC has been proven [27] to provide solutions of the Boltzmann equation for all Knudsen numbers, we expect validation at the two Knudsen extremes to be sufficient.

A typical metric used in quantifying CVD is the *Step Coverage* defined in this paper as the ratio of the thickness of the deposited film at the location of interest to the thickness of the deposited film on a flat surface (typically measured outside and as far as possible from the trench – see Fig. 1). Step coverage is particularly useful for describing the conformality of the deposited layer, in the sense that a step coverage close to 1 denotes conformal deposition whereas a step coverage close to 0 denotes a non-conforming deposition. The step coverage can be measured at various locations; the most common are the bottom step coverage (b/a in Fig. 1) also typically referred to as step coverage, and the corner step coverage which quantifies the film growth in the trench bottom corners. The trench *aspect ratio* (AR) is defined here as ratio of the initial trench depth to the initial width of the trench mouth.

3.1. Validation in the $Kn\to\infty$ limit

In this section we compare our results to previously published data obtained using an independently developed, high Knudsen number method known as EVOLVE [22]. The chemistry model used is identical to the one used in [13], that is, a reaction of the form

$$WF_6+3H_2\to W(s)+6HF \tag{9}$$

and a rate equation of the form

$$\mathscr{R}_{WF_6}=\text{Constant}(T)\sqrt{pp_{H_2}}\left(\frac{pp_{WF_6}}{pp_{WF_6}^{\text{bulk}}}\frac{1+C\,pp_{WF_6}^{\text{bulk}}}{1+C\,pp_{WF_6}}\right), \tag{10}$$

where C is a constant and pp_i^{bulk} is a reference pressure taken to be the pressure at the top of the trench.

Fig. 2 presents a comparison of results. The plot on the left shows the closure step coverage (bottom step coverage evaluated when the growth surface pinches off) as a function of the deposition temperature for low pressure Tungsten CVD. On the right we show a plot of the closure step coverage for the same model with a variable trench aspect ratio at a fixed temperature. The comparison shows that except from the statistical noise inherent in DSMC, the solutions are in excellent agreement, in the presence of non-trivial chemistry and variable temperature. In Fig. 3 we compare our predictions for the step coverage versus the sticking

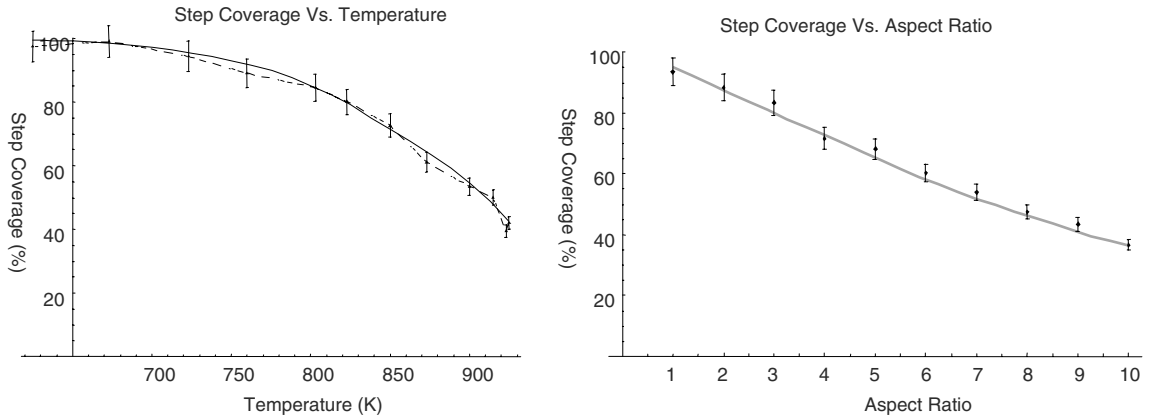

Fig. 2. Validation in the limit $Kn \to \infty$. Our results are denoted by symbols and the results of [22] are shown in a continuous line. The left plot shows the step coverage (at closure) for a square trench ($AR = 1$) over a wide range of temperatures. The right plot is of the step coverage (at closure) at a deposition temperature of 723 K for trenches of various aspect ratios.

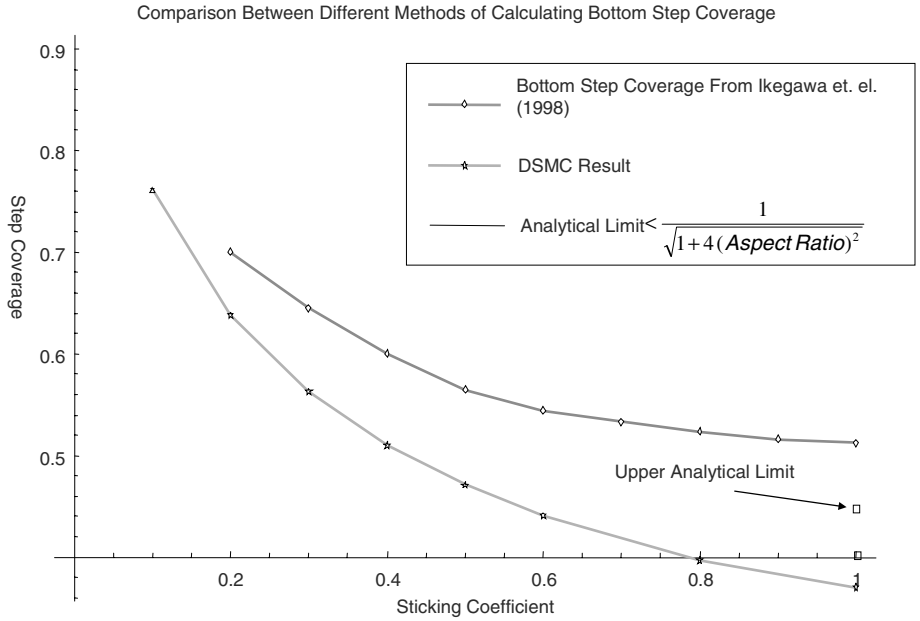

Fig. 3. Results for step coverage versus the sticking coefficient for a square trench at $Kn \to \infty$. The results by Ikegawa et al. are transcribed from [23]. The analytical result shown for $Sc = 1.0$ is an upper bound [14] for the step coverage.

coefficient for a square trench ($AR = 1$) with those from [23]. The step coverage is evaluated when a (see Fig. 1) is equal to half the trench depth. The analytical result indicated in the figure serves as an upper bound for the step coverage for $Sc = 1.0$ (see [14] for details). The comparison suggests that previous results may not be very reliable.

3.2. Low Knudsen number results

The previous tests establish that both surface chemistry and collisionless transport are captured correctly by our model. As stated above, DSMC solutions become computationally expensive as the Knudsen number approaches zero. Thus, to examine the effect of collisions on transport, we devised the following

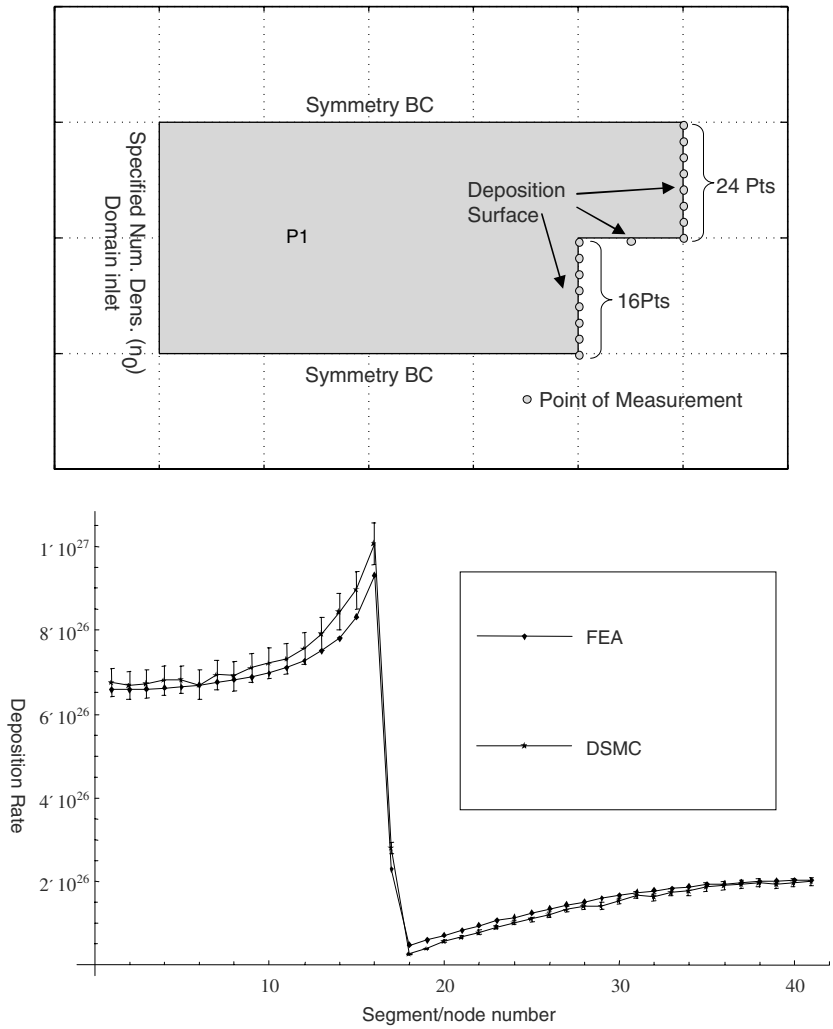

Fig. 4. Validation for $Kn = 0.03$. Top: Sketch of computational domain along with boundary conditions and measurement points. Bottom: Plot of the finite element analysis (FEA) solution and DSMC results for the deposition rate as a function of position. The deposition rate is in particles per square meter per second.

test. We obtained a solution using our methodology for the lowest Knudsen number ($Kn = 0.03$) we could achieve using our computational resources. We then compared this result to a finite element solution of the diffusion equation; the latter is expected to provide a benchmark solution for $Kn \to 0$. The sticking coefficient was taken to be constant in both calculations.

Fig. 4 shows a comparison between our results and those obtained from the diffusion equation solution. The top plot shows a sketch of the diffusion domain along with the location of nodes where results are collected. The bottom plot compares the results of our DSMC model with the continuum model results. The agreement between the two models is very good, confirming that our model does indeed capture the physics of transport at low *Kn* numbers [14].

3.3. Transition regime results

We finally present and discuss some general trends that our methodology predicts for a simple square trench in the transition regime. Fig. 5 shows a plot of the ratio of the deposition rate at the top and center of the trench (the *Flux Step Coverage*) for a large number of different sticking coefficients at different values of the Knudsen number. Clearly, the conformality of the deposited layer improves as the Knudsen number increases at all finite values of the sticking coefficient which agrees with previous results [10]. Furthermore, it is clear that the step coverage is a strong function of both the sticking coefficient and the Knudsen number and no general simplification can be made that would allow us to ignore the transport effects at intermediate *Kn* values.

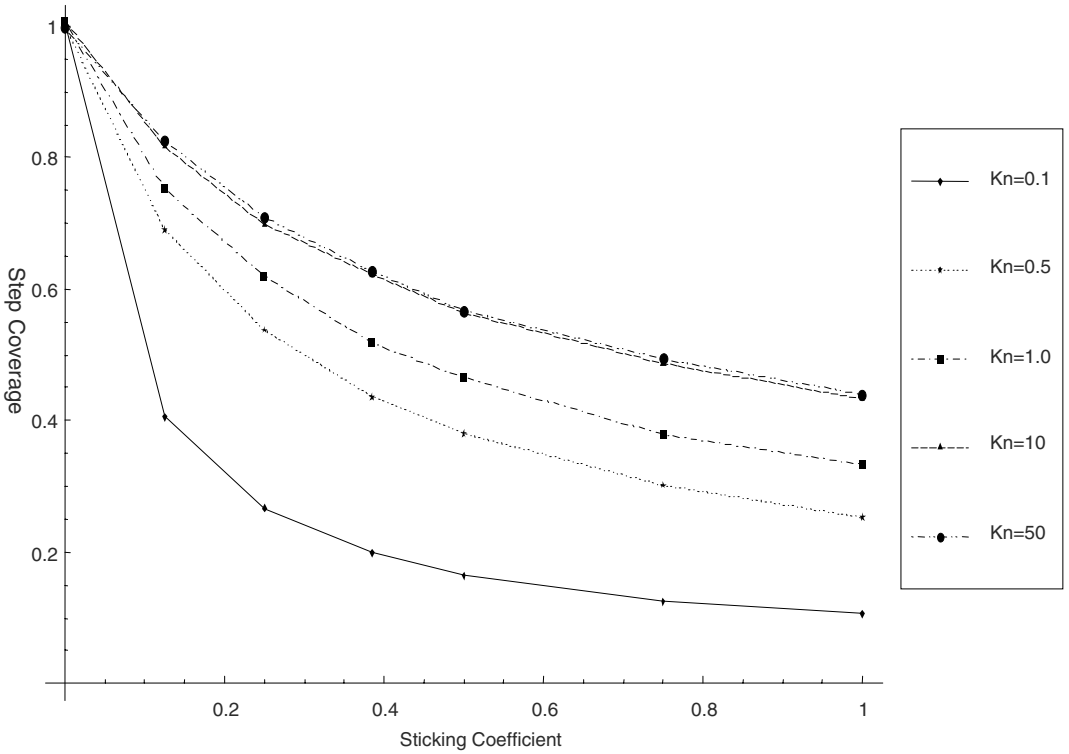

Fig. 5. Flux step coverage at base versus *Kn* and sticking coefficient for a square ($AR = 1$) trench.

4. Conclusion

We have presented a methodology for modeling CVD at arbitrary Knudsen numbers. This was made possible by using DSMC as the transport model. In this work, DSMC was endowed with a surface evolution model based on level set theory. Furthermore, we presented a method to account for complex surface chemistry which utilizes surface sticking coefficients that vary in both space and time. Our methodology was applied to a number of problems to generate results that have been verified at both the diffusive and ballistic limit.

This work can be extended in a number of different directions. A worthwhile extension would be the addition of weighting factors in the DSMC formulation [2] to capture CVD reactions with low concentrations of reacting species. Weighting factors have been reported to cause random walks [2]; however, some methods have been proposed to alleviate those [25]. Extension to 3D problems also poses interesting challenges. Both current DSMC and level set implementations can be extended to three dimensions; the computational cost of three-dimensional calculations, however, is expected to be considerable. Finally, direct comparison with experimental data in the transition regime will be pursued.

Acknowledgements

The authors would like to thank Lowell Baker for help with the manuscript preparation and Drs Maria Nemirovskaya and Pauline Ho as well as Professor Klaus Jensen for valuable comments and discussions. This work was supported, in part, by ASML (thermal division) and the Saudi Arabian Oil Company.

References

[1] T.S. Cale, D.F. Richards, D.W. Tang, Opportunities for materials modeling in microelectronics: programmed rate chemical vapor deposition, J. Comput. Aided Mater. Des. 6 (1999) 283–309.
[2] G.A. Bird, Molecular Gas Dynamics and the Direct Simulation of Gas Flows, Oxford University Press, Oxford, 1998.
[3] J.O. Hirschfelder, C.F. Curtiss, R.B. Bird, Molecular Theory of Gases and Liquids, Wiley, New York, 1964.
[4] T.S. Cale, T.P. Merchant, L.J. Borucki, A.H. Labun, Topography simulation for the virtual wafer fab, Thin Solid Films 365 (2000) 152–175.
[5] M.M. IslamRaja, M.A. Cappelli, J.P. McVittie, K.C. Saraswat, A 3-dimensional model for low-pressure chemical vapor deposition step coverage in trenches and circular vias, J. Appl. Phys. 70 (11) (1991) 7137–7140.
[6] H. Liao, T.S. Cale, Low-Knudsen-Number transport and deposition, J. Vac. Sci. Technol. A 12 (4) (1994) 1020–1026.
[7] W. Pyka, P. Fleischmann, B. Haindl, S. Selberherr, Three-dimensional simulation of HPCVD: linking continuum transport and reaction kinetics with topography simulation, IEEE Trans. Comput. Aided Des. IC Syst. 18 (12) (1999) 1741–1749.
[8] Y. Akiyama, S. Matsumura, N. Imaishi, Shape of film grown on microsize trenches and holes by chemical vapor deposition: 3-dimensional Monte Carlo simulation, JPN. J. Appl. Phys. 34 (11) (1995) 6171–6177.
[9] D.G. Coronell, Simulation and analysis of rarefied gas flows in chemical vapor deposition processes, Ph.D. Dissertation, MIT, 1993.
[10] M.J. Cooke, G. Harris, Monte Carlo simulation of thin-film deposition in a rectangular groove, J. Vac. Sci. Technol. A 7 (6) (1989) 3217–3221.
[11] D.G. Coronell, K.F. Jensen, Simulation of rarefied-gas transport and profile evolution in nonplanar substrate chemical-vapor deposition, J. Electrochem. Soc. 9 (141) (1994) 2545–2551.
[12] M. Ikegawa, J. Kobayashi, Development of a rarefied gas flow simulator using the direct-simulation Monte Carlo method, JSME Int. J. II 33 (3) (1990) 463–467.
[13] T.S. Cale, T.H. Gandy, G.B. Raupp, A fundamental feature scale model for low pressure deposition process, J. Vac. Sci. Technol. A 9 (3) (1991) 524–529.
[14] H.A. Al-Mohssen, Chemical vapor deposition models using direct simulation Monte Carlo with non-linear chemistry and level set profile evolution, SM Dissertation, MIT, September 2003.
[15] F.J. Alexander, A.L. Garcia, The direct simulation Monte Carlo, Comput. Phys. 11 (6) (1997) 588–593.

[16] E.S. Oran, C.K. Oh, B.Z. Cybyk, Direct simulation Monte Carlo: recent advances and applications, Annu. Rev. Fluid Mech. 3 (1998) 403–441.
[17] T.S. Cale, V. Mahadev, Low pressure deposition processes, in: S. Rossnagel, A. Ulman (Eds.), Thin Films, 22, Academic Press, 1996, pp. 172–271.
[18] S. Osher, J.A. Sethian, Fronts propagating with curvature-dependent speed: algorithms based on Hamilton–Jacobi formulations, J. Comput. Phys. 79 (1988) 12–49.
[19] J.A. Sethian, Level Set Methods and Fast Marching Methods: Evolving Interfaces in Computational Geometry, Fluid Mechanics Computer Vision and Materials Science, Cambridge University Press, Cambridge, 1999.
[20] D.F. Richards, M.O. Broomfield, S. Sen, T.S. Cale, Extension velocities for level set based surface profile evolution, J. Vac. Sci. Technol. A 19 (4) (2001) 1630–1635.
[21] J. Sethian, D. Adalsteinsson, An overview of level set methods for etching deposition and lithography development, IEEE Trans. Semiconduct. Devices 10 (1) (1997) 167–184.
[22] M.K. Jain, Maximization of step coverage at high throughput during low-pressure deposition process, Ph.D. Dissertation, Arizona State University, 1992.
[23] M. Ikegawa, J. Kobayashi, M. Maruko, Study on the deposition profile characteristics in the micron-scale trench using direct simulation Monte Carlo method, Trans. ASME Fluids Eng. Div. 120 (1998) 296–302.
[24] I.D. Boyd, D. Bose, G.V. Candler, Monte Carlo modeling of nitric oxide formation based on quasi-classical trajectory calculations, Phys. Fluids 9 (4) (1997) 1162–1170.
[25] I.D. Boyd, Conservative species weighting scheme for the direct simulation Monte Carlo method, J. Thermophys. Heat Transfer 10 (4) (1996) 579–585.
[26] H.S. Wijesinghe, N.G. Hadjiconstantinou, Hybrid atomistic-continuum methods for multiscale hydrodynamics, to appear in the International Journal of Multiscale Computational Engineering.
[27] W. Wagner, A convergence proof for Bird's direct simulation Monte Carlo method for the Boltzmann equation, J. Stat. Phys. 66 (1992) 1011–1044.
[28] F.J. Alexander, A.L. Garcia, B.J. Alder, Cell size dependence of transport coefficients in stochastic particle algorithms, Phys. Fluids 10 (1998) 1540–1542, Erratum: Phys. Fluids 12 (2000) 731.
[29] N.G. Hadjiconstantinou, Analysis of discretization in the direct simulation Monte Carlo, Phys. Fluids 12 (2000) 2634–2638.
[30] A.L. Garcia, W. Wagner, Time step truncation error in direct simulation Monte Carlo, Phys. Fluids 12 (2000) 2621–2633.
[31] W.H. Press, S.A. Teukolsky, W.T. Vetterling, B.P. Flannery, Numerical Recipes in C, second ed., Cambridge University Press, Cambridge, 1992.